Entropy and attractor dimension as measures of the field-atom interaction

R. P. Frueholz and J. C. Camparo

Electronics Technology Center, The Aerospace Corporation, P.O. Box 92957, Los Angeles, California 90009

We have examined the population oscillation amplitudes, associated attractors, and the order-1 Renyi entropy of Bloch-vector trajectories for a two-level atom interacting with an electromagnetic field, whose phase varies in a two-frequency quasiperiodic manner. Distinct differences in these quantities are observed as the strength of the exciting field varies from weak (nonadiabatic dynamics) to strong (adiabatic dynamics). We find, though, an underlying homology. In all cases the response is two-frequency quasiperiodic with a resulting two-dimensional attractor for the quantum system. Additionally, correlated with observed Rabi resonances, there are abrupt increases in the entropy of the system. A key finding is that Rabi resonances are more than simple increases in the amplitude of a quantum system's population oscillations; the atomic dynamics abruptly becomes more disordered at these resonances.

I. INTRODUCTION

The response of a simple quantum-mechanical system to a quasiperiodic electromagnetic perturbation is an area of much present activity. Initially, interest in this area was generated by a motivation to understand better the phenomenon of quantum chaos [1]. Now, however, it is recognized that independent of chaos (quantum or classical), atomic interactions with quasiperiodic perturbations result in novel dynamical features, interesting in their own right. An atom's response to a quasiperiodic field is often extremely complex, and techniques developed to characterize chaos have been fruitfully applied to the study of these complicated quantum-mechanical dynamics [2]. Specifically, a number of authors have investigated atomic systems subjected to electromagnetic fields with quasiperiodic amplitude modulation [2,3], and have found that the atomic density-matrix elements have rapidly decaying autocorrelation functions.

In a previous paper (to be referred to as I), we analyzed the dynamics of a two-level atom subjected to a field whose *phase* variation was quasiperiodic: a superposition of a sinusoid and a square wave with the frequencies chosen to be incommensurate [4]. In the present work, we have continued to utilize the analytical techniques of nonlinear dynamics in the study of complicated, albeit not classically chaotic (lacking positive Lyapunov exponents) atomic dynamics. We have investigated the response of a two-level atom to a field with a simpler form of phase modulation, two sinusoids with incommensurate frequencies. For this simpler form of modulation, the time scale of phase variations is well defined, and hence adiabatic and nonadiabatic quasiperiodic perturbations can have clearer meanings. In the case of square-wave modulation, the phase changes instantaneously, and thus the time scale of the phase variations can never be slower than the time scale associated with the field-atom interaction. As in I, the atomic dynamics are studied as a function of the perturbing field strength, which can be thought of as a control parameter. Here,

however, the dynamics are characterized through the computation of Bloch-space entropies in addition to attractor dimensions. Furthermore, we compute Bloch-vector trajectories in a reference frame defined by the phase of the field, which is related to the standard rotating frame of radiation problems by an instantaneous transformation in the rotating frame's XY plane. Though the atomic dynamics can be extremely complicated, the three-dimensional (3D) portraits of the Bloch-vector trajectories in this instantaneous frame yield relatively simple geometrical entities.

Our results demonstrate that even though the atomic population dynamics are erratic in the quasiperiodic field, the atom's behavior can nonetheless be quantified by the above-mentioned measures. We find that in general, the 3D portraits of Bloch-vector trajectories can be described as one of three distinct geometrical objects depending on whether the dynamics are classified as nonadiabatic, transitional (i.e., between nonadiabatic and adiabatic), or adiabatic. The entropy associated with these Bloch-space attractors peaks in the transitional regime, and moreover shows enhancements at the Rabi resonances. Finally, regardless of how the entropy and Bloch-space attractors change with field strength, our results show that there is a homology to the dynamics that is manifested in the quantum system's Hausdorff dimension D_0. In all cases of this two-frequency (incommensurate) quasiperiodic perturbation that we have examined, we find evidence that $D_0 = 2$, and we believe that in all these cases the quantum system attractor is homeomorphic to a 2-torus.

II. DESCRIPTION OF SYSTEM UNDER ANALYSIS

To describe the atom's response to the field we employed the optical Bloch equations (i.e., two-level atom density-matrix equations) (1a)–(1c) including phenomenological relaxation rates γ_1 and γ_2 [5]:

$$\dot{X} = -\gamma_2 X - \Delta Y + \Omega Z \sin[\theta(t)] , \qquad (1a)$$

$$\dot{Y} = \Delta X - \gamma_2 Y + \Omega Z \cos[\theta(t)] \ , \tag{1b}$$

$$\dot{Z} = -\Omega X \sin[\theta(t)] - \Omega Y \cos[\theta(t)] + \gamma_1 (Z_0 - Z) \ . \tag{1c}$$

In these equations Ω is the Rabi frequency, Δ is the detuning of the field from resonance, and X, Y, and Z are the coordinates of the Bloch vector in the rotating coordinate frame. Under steady-state conditions the Bloch vector precesses about an effective field, whose orientation in the rotating coordinate frame's XY plane is described by the angle θ. As noted in I the inclusion of relaxation in the optical Bloch equations insures that the atomic dynamics will, after a sufficient period of time, reach an attractor.

In order for the field variations to be nontrivial, yet to have a well-defined time scale, the field's time-dependent phase was given by

$$\theta(t) = \theta_1(t) + \theta_2(t) = \pi \sin(\omega_1 t) + \pi \sin(\omega_2 t) \ . \tag{2}$$

Two incommensurate modulation frequencies were typically employed, with ω_2 equal to ω_1 multiplied by five times the golden mean [golden mean $=(\sqrt{5}-1)/2$], with $\omega_1 = 10.0$, $\omega_2 = 30.90 \ldots$. This choice of relative modulation frequencies insured that their ratio was strongly irrational [6]. The number of phase-space variables associated with the atomic dynamics is the sum of the three associated with the Bloch space and contributions from the modulation frequencies. For incommensurate modulation frequencies each frequency contributes one phase-space variable to the sum [7]. Consequently, our analysis dealt with five-dimensional phase spaces for the full dynamics of the atomic system.

Following the procedures of I the time scale was normalized to the intrinsic relaxation time $1/\gamma$ ($\gamma = \gamma_1 = 2\gamma_2$), Δ was taken as 0, $Z_0 = -1$ [4]. The equations were solved using a fourth-order Runge-Kutta algorithm with adaptive step size. In the present analysis, step size was controlled by requiring the relative error in the computation of any Bloch-vector component at each step to be less than 10^{-11}. To insure that transients had died away, and that the computed trajectory had reached the attractor, the solution was propagated to $t = 12$ prior to accumulating data. Typically, 50 000 arbitrarily chosen data points were collected between $t = 12$ and 100, so that roughly 10^2 cycles of the long period θ_1 oscillation were sampled and about 10^2 data points were distributed over the short θ_2 period.

III. RESULTS

A. Rabi resonances and attractor dimensions

As a first step in analyzing the response of the atomic system, Bloch-vector trajectories were calculated for a range of field strengths. We found that the three-dimensional plots of Bloch-vector trajectories were most informative when viewed in the instantaneous reference frame described by Avan and Cohen-Tannoudji [8]. In this frame, the X' axis is taken along the direction of the effective field [i.e., $\theta(t)$], rather than along a fixed direction in the rotating frame (i.e., $\theta = 0$). As our calculations

employed $\Delta = 0$, only a simple, time-dependent rotation of the X and Y components, generated by solution of Eqs. (1a)–(1c), was required to produce the X' and Y' coordinates of the instantaneous frame. The advantage of viewing the dynamics in the instantaneous frame is that the orientation of the effective field is a constant in this frame, and so attention is focused on the atomic variables of interest; the trivial angular variations associated with $\theta(t)$ are removed from the Bloch-vector trajectories by the coordinate system transformation.

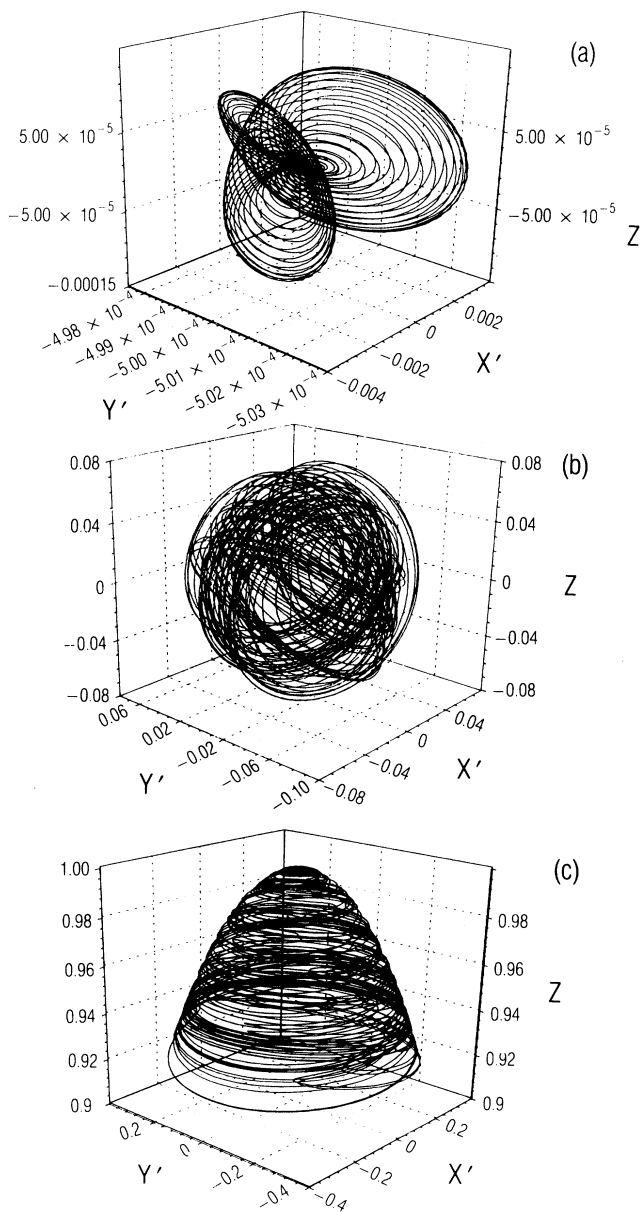In Fig. 1 we display the Bloch-space attractors for

FIG. 1. Bloch-space attractors in the three-dimensional, instaneous frame. Two incommensurate frequencies (10.0 and 30.9 . . .) employed for phase modulation as per Eq. (2). (a) Adiabatic atomic response $\Omega = 2000$; (b) transitional response $\Omega = 100$; (c) nonadiabatic response $\Omega = 1$.
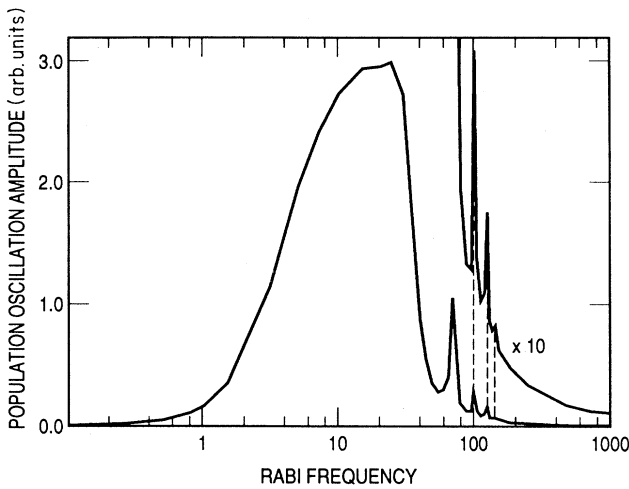
FIG. 2. Amplitude of population oscillations as a function of Rabi frequency.

three different field strengths. The phase of the field was modulated according to Eq. (2) with two incommensurate frequencies. With a Rabi frequency of 2000 [Fig. 1(a)] we obtain the system's nominal strong field, adiabatic response. The basic pattern of adiabatic trajectories shown in the figure is essentially independent of field strength for Rabi frequencies above 500, though its absolute size becomes smaller as the Rabi frequency is increased. The system's nominal weak-field nonadiabatic response is obtained at a Rabi frequency of 1 [Fig. 1(c)].

The basic pattern of nonadiabatic trajectories is unchanging for Rabi frequencies below 2, while the absolute size again decreases with decreasing Rabi frequency. In the transition regime between the adiabatic and nonadiabatic dynamics, a highly disordered pattern of trajectories in Bloch space results. For a single modulating frequency, we have also found that the pattern of trajectories changes significantly in shifting from the strong- to weak-field regimes of atomic dynamics. However, as one might expect, the trajectories lack the complexity observed with two incommensurate modulation frequencies.

Cappeller and Mueller [9] have recognized that, when an atomic system is exposed to a driving field with a particular modulation pattern (like ours), abrupt increases in the amplitude of population oscillations are often observed at specific Rabi frequencies. These increases are referred to as "Rabi resonances" [9,10]. In Fig. 2 we display the magnitude of the population oscillations, the difference between the maximum and minimum attractor Z values, as a function of Rabi frequency. Several sharp features ($\Omega = 142$, 125, 100, and 70), as well as a broad amplitude enhancement (peaking at $\Omega = 25$) are observed in or about the dynamical transition region. In Fig. 3 we display the Bloch-space attractors across the transition region. Of particular interest is the abrupt alteration of the trajectories between the Rabi frequencies of 90 and 110 associated with the sharp feature at $\Omega = 100$ of Fig. 2: the trajectories appear more disordered at $\Omega = 100$, and the mean value of the Y coordinate has shifted from a negative value to zero. These figures clearly show that a Rabi resonance not only affects the amplitude of the os-
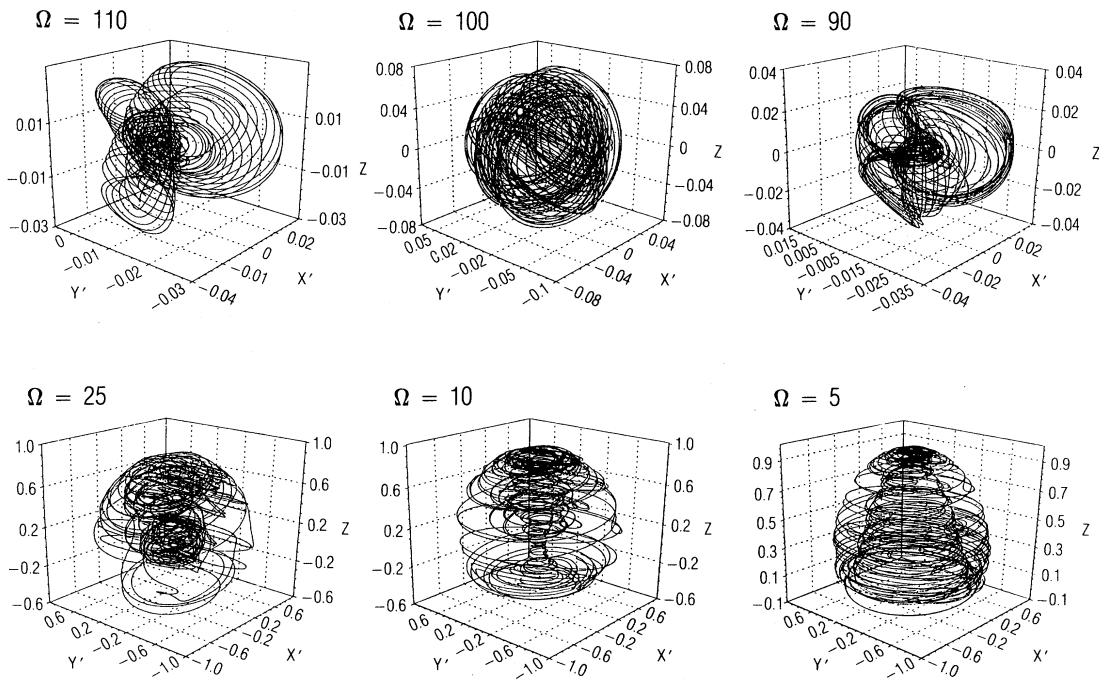

FIG. 3. Bloch-space attractors for Rabi frequencies in the transition region. The abrupt change in dynamics between $\Omega = 90$ and 110 represents an entropy resonance. Additionally there is a gradual evolution in the system dynamics from the primarily adiabatic response observed at $\Omega = 110$ to the largely nonadiabatic response observed for $\Omega = 5$.

cillation, but also the details of the Bloch vector's trajectory.

To better understand the specifics of the dynamics under adiabatic and nonadiabatic conditions of interaction, as well as the extremely complex behavior at Rabi resonances, we have calculated generalized dimensions of our quantum system attractors using the generalized correlation integral approach discussed by Pawelzik and Schuster [11]. Of particular relevance to our following discussion are D_0, D_1, and D_2, the Hausdorff, information, and correlation dimensions, respectively. Attractors in the full five-dimensional space were studied, with the atomic variables obtained from the rotating coordinate frame (i.e., foregoing the time-dependent transformation leading to the instantaneous frame). However, initial attempts to directly analyze attractor dimensions in the five-dimensional space were unsuccessful: with a tractable 50 000 points spread over the attractor, systematic misestimates of dimension resulted.

To reduce the dimension of the entity to be analyzed, while preserving the information of the full five-dimensional attractor, a two-step process was employed. As the first step, we projected the five-dimensional attractors onto a three-dimensional space. From the projection theorem [12], we know that for a projection onto almost any (in a measure theoretic sense) three-dimensional space, the Hausdorff dimension of the projected set will be the same as that of the initial set if the dimension of the attractor in the five-dimensional space is less than or equal to 3. By proceeding in this direction, a tacit assumption is made that the dimensions of the full attractors are indeed less than 3. This is confirmed at the conclusion of the calculation. The basis vectors for the three-dimensional space e_1, e_2, and e_3 $(1, -1, 1, -1, 1)$, $(4, 6, 4, 1, -1)$, $(0, 0, 0, 1, 1)$ $(X, Y, Z, \theta_1, \theta_2)$, were obtained via the Gram-Schmidt procedure from three linearly independent vectors $(1, -1, 1, -1, 1)$, $(1, 1, 1, 0, 0)$, $(0, 0, 0, 1, 1)$, which together reflected both angular and atomic character. Projections were also made onto other three-dimensional spaces with no substantive effect on the dimension calculations. Application of the intersection theorem [12] further reduces the dimension of the analysis. For almost any nonempty intersection between a simple plane and the projected set, the Hausdorff dimension of the projected set will be equal to that of the intersection plus unity. Consequently, adding one to the Hausdorff dimension of this intersection should produce the dimension of the full five-dimensional attractor. The plane employed to generate the intersection set was defined by requiring its projection onto e_1 to equal the average value of the e_1 component for the projected set.

Prior to performing the correlation integral analysis, much information concerning the system's dynamics was obtained by direct inspection of the intersection sets. Badii and Meier [2] have used this simple approach to demonstrate that the complicated response of a two-level quantum system to a bichromatic exciting field is quasiperiodic rather than chaotic. In Fig. 4, 4096 points from the intersection sets for Rabi frequencies of 2000 and 1 are presented. The sets appear one dimensional, indicating the full response of the system in either limiting case
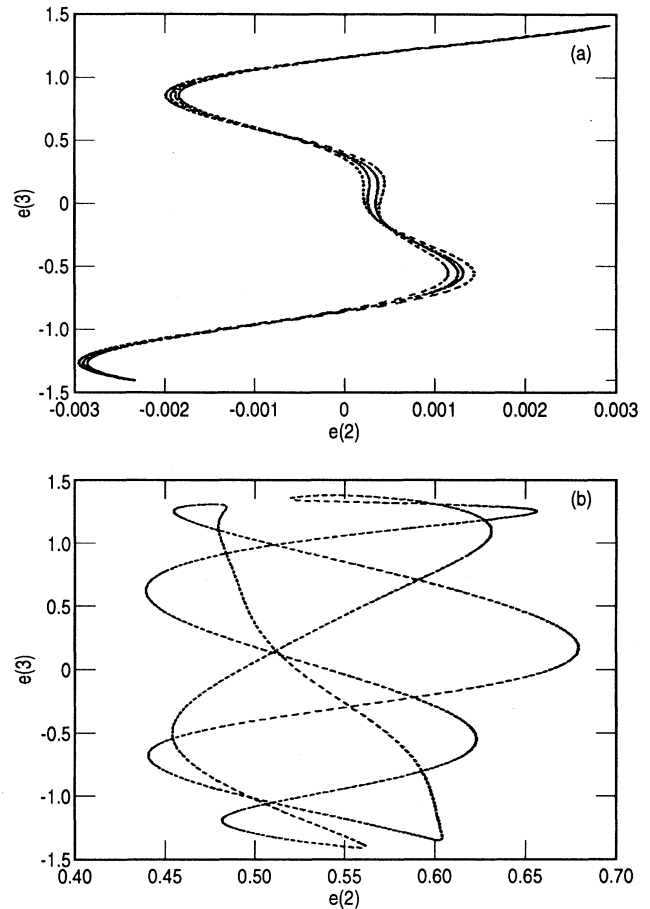

FIG. 4. Intersection sets (see text for definition). (a) $\Omega = 2000$; (b) $\Omega = 1$.

is two dimensional (i.e., $D_0 = 2$). The intersection set for the case of a Rabi resonance ($\Omega = 100$) is similarly one dimensional. Additionally, following Romeires and Ott [13], stroboscopic sections generated by plotting the Z component of the Bloch vector $Z(t_n)$ versus $\Gamma(t_n) = \omega_1 t_n \bmod(2\pi)$ with $t_n = 2\pi n / \omega_2 + 12$ were simple one-dimensional curves for each of the three cases. Our results then suggest that the motion is always two-frequency quasiperiodic, independent of whether the dynamics are classified as nonadiabatic, transitional, or adiabatic.

On close inspection, the intersection sets appear nonuniform, which warrants the calculation of their generalized dimensions D_q. For this task, the generalized correlation integral approach was applied using 50 000 points from each intersection. The resulting generalized dimensions for Rabi frequencies equal to 1 and 2000 are presented in Fig. 5. For the adiabatic case D_0 is found to be 0.98 ± 0.03, consistent with the expectation that the dimension of the full attractor is 2. Error bars express our confidence in the D_q value, which in part is limited by our ability to find the appropriate linear portion of the log[correlation integral]'s dependence on the log of the scaling length. However, the clear change in dimension
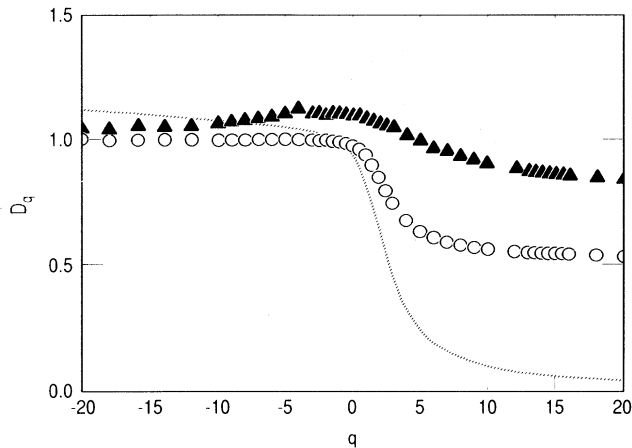
FIG. 5. Generalized dimensions obtained from analysis of the intersections sets of Fig. 4. Circles, $\Omega = 2000$, and triangles, $\Omega = 1$. The dashed line represents generalized dimensions, reduced by unity, of a set with coordinates defined by the angular variables $\sin(\omega_1 t)$ and $\sin(\omega_2 t)$.

with q shows quantitatively that at least the intersection set and probably the full attractor have multifractal characteristics. (We note parenthetically that nonuniform attractor coverage implies that $D_2 \neq D_0$, and consequently that a noninteger value of D_2 cannot be taken as evidence of a strange attractor as hypothesized in I [4].) In Fig. 5, the triangles are the generalized dimensions for the nonadiabatic case. Even after reducing the dimension of the analysis to two, we obtain a relatively high value for D_0, 1.10, which we believe is systematically too large by 10%. This error arises from difficulties in fitting the correlation integral data to straight lines for certain values of q, and so for the nonadiabatic case it is our contention that the entire range of dimensions suffers from a systematic offset no larger than about 10%. Nevertheless, it is clear that in the nonadiabatic regime the D_q do not vary as significantly with q as they do in the adiabatic regime. Attempts to calculate the generalized dimensions when the Rabi frequency was 100 were not particularly successful, though D_0 was found to be 1.15, similar to the nonadiabatic case.

The nonconstant D_q obtained from these sets could derive from an underlying multifractal characteristic in the system under study, or they could merely be the result of some distortion introduced by the projection procedure. If the latter is the case, then the observation of nonconstant D_q has little physical significance. This explanation, however, is unlikely. The variations in D_q appear to derive from the characteristics of the phase modulation pattern. This is demonstrated by the dashed line in Fig. 5, which shows the generalized dimensions, all reduced by unity, of 50 000 points selected from the $[\theta_1, \theta_2]$ trajectory. The value of D_0 for this set is found to be 2.0, consistent with our expectations, while the limiting values of D_q as $q \to -\infty$ and $q \to +\infty$ are ~ 2.2 and ~ 1.1, respectively. The phase modulation pattern thus provides an underlying multifractal characteristic in the system that is still apparent in the intersection sets.

In itself the multifractal nature of the phase modulation pattern may be unexpected. However, the following observations, while not unambiguous, shed light on the issue. Simple D_q calculations performed on the two-dimensional points $[\theta_1, \sin(\theta_1)]$, with θ_1 distributed uniformly between 0 and 2π, confirm an expected value of unity for all D_q's. When similar calculations are performed in one dimension on only the $\sin(\theta_1)$ values, though, a nonconstant set of D_q's is obtained, with $D_q = 1$ for $q \leq 0$ and $D_q = 0.5$ as q goes to $+\infty$. Using the definition of D_q (Ref. [14]), simple analytical manipulations may be performed in limiting cases for the one-dimensional example, and these yield the same results: $D_{-\infty} = D_0 = 1$ and $D_{+\infty} = 0.5$. Since nonconstant values of D_q result from the analysis of $\sin(\theta_1)$, it is probably not surprising that nonconstant D_q's are obtained in our two-dimensional case with the points defined by $(\sin(\theta_1), \sin(\theta_2))$. We consider this, however, far from a definitive explanation, and therefore a topic for future investigation.

Given that the attractors, analyzed in the rotating frame, were found to have geometries to which the θ_1 and θ_2 variables make significant contributions, it remains to be seen what contributions the atomic variables by themselves make to the attractors of the system. In going from the laboratory frame to the rotating frame the problem has been moved from a stationary frame to one that rotates uniformly in time, independent of any comparatively slow phase modulations that might be applied. In this manner, uniform rapid rotation of the X and Y Bloch-vector components is removed from the problem. In contrast, transformation into the instantaneous frame has dynamical significance. The nonuniform nature of this rotational transformation is derived from the variations in the phase modulation variables, quantities of dynamical interest. Therefore, we anticipate that the gross effects of the angular variables can be removed by a transformation to the instantaneous frame, allowing more detailed inspection of the dynamics resulting from the atomic portion of the system.

In Fig. 6 we show generalized dimensions produced by the analysis of 50 000 points from the intersection of the three-dimensional Bloch-space attractors in the instantaneous frame and a plane defined by the average value of $Z(t)$ for each Rabi frequency. The adiabatic, high Rabi frequency response shows generalized dimensions virtually independent of q, indicating that the "residual" atomic motion generates a uniformly covered, two-dimensional attractor. We attributed this behavior to the fact that under adiabatic conditions the Bloch vector follows the motion of the angular variables of the field very closely. By going into the instantaneous frame, under adiabatic conditions, this angular motion is removed virtually entirely from the system and with it the underlying multifractal nature. In contrast, under nonadiabatic conditions, as shown in Fig. 6, the atomic motion still maintains multifractal characteristics, with D_0 again equal to 2. Under these conditions the Bloch vector does not closely follow the angular variations. The attempt to remove the effects of the angular variables through transformation to the instantaneous frame is ineffective and in-
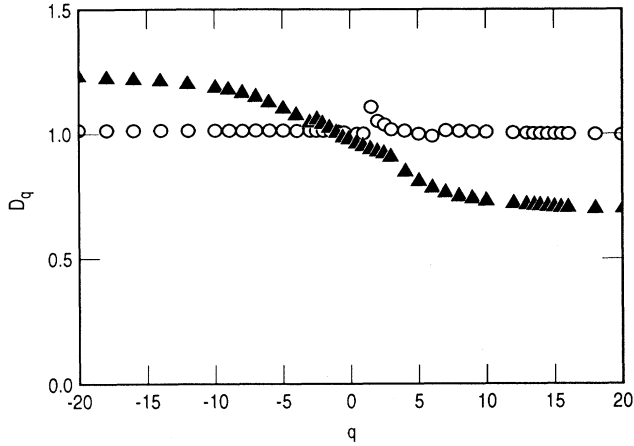
FIG. 6. Generalized dimensions of intersection sets formed by Bloch-space attractors in the instantaneous frame and a plane defined by Z equals the average value of $Z(t)$. Circles, $\Omega = 2000$, and triangles, $\Omega = 1$. At present we do not have a good explanation for the discontinuity in the D_q values that occurs at $q = 1.5$ for $\Omega = 2000$

dications of a multifractal remain. Consequently, our findings are consistent with the multifractal nature being a true characteristic of this system (not an artifact of the generalized dimension analysis procedures) with its origin in the phase modulation pattern.

In the absence of phase variations and in steady state, the attractor for the Bloch-vector trajectory in the rotating frame is a point. Naively, when phase variations are introduced into the field, one might imagine that in the instantaneous frame the attractor would also be a point, since the Bloch vector follows the effective field in the adiabatic regime, and the orientation of the effective field is a constant in this frame. An attractor with zero dimension in the instantaneous frame would suggest that the transformation to this frame has allowed the atom–phase-varying-field problem to be couched in the steady-state form of an atom's interaction with a monochromatic field. Our results, however, show this to be untrue. Even though the volume that the Bloch-space attractor encloses in the adiabatic regime shrinks as the field strength gets ever larger, the Bloch-vector trajectories remain confined to a surface. This in turn implies that even for infinitely large field strengths, there is no coordinate frame which can be chosen to trivialize the atom–phase-varying-field interaction problem: *there is no coordinate frame which will allow the radiative problem to be solved exactly by considering a monochromatic field inducing steady-state Bloch-vector components.*

B. Entropy calculations

While the basic nature of the atomic system's response is independent of the Rabi frequency, it is apparent from the Bloch-space attractors that the precise nature varies with field strength. Crudely, the trajectories in the instantaneous frame appear more complicated in the transition region and particularly near a Rabi resonance. To

provide a quantitative measure of the change in the complexity of the Bloch-vector trajectories observed in the instantaneous frame, we calculated the order-1 Renyi entropy (sometimes referred to as the Shannon information or entropy). This is in contrast to the Kolmogorov entropy which is more closely related to the dynamical characteristics of the atomic system's phase-space trajectories [15]. The order-1 entropy was chosen for study, since it has a close similarity to the standard statistical thermodynamic entropy [16] and as such may be thought of as a measure of the trajectory's "disorder." The evaluation of entropy was performed via a simple box counting method. Laying grids of approximately 10^6 cubes with sides ϵ over the Bloch-space attractors, the probability of a point on the trajectory falling in the ith cube p_i was calculated. The entropy is then given by

$$S_{R1}(\epsilon) = \sum_{i=1}^{N(\epsilon)} p_i \ln(p_i) . \tag{3}$$

As the absolute sizes of the attractors, hence box dimensions, vary, the values of $S_{R1}(\epsilon)$ cannot be directly compared. To provide a scale-independent measure of complexity $S_{R1}(0)$ was calculated for each Rabi frequency employing [15]

$$S_{R1}(0) = S_{R1}(\epsilon) + D_1 \ln(\epsilon) . \tag{4}$$

The generalized dimension calculations for adiabatic conditions ($\Omega = 2000$), to which we assess our highest confidence, yielded a value for D_1 of 1.94. As our results indicate that D_1 is nearly constant relative to D_0 (perhaps changing by $\sim 3\%$) for all Rabi frequencies, we used the same value of 1.94 for D_1 in all cases.

Entropies for the Bloch-vector trajectories along with the oscillation amplitudes are displayed in Fig. 7. The transition region, as might be inferred from Figs. 1 and 3, displays an increased entropy relative to strong- and
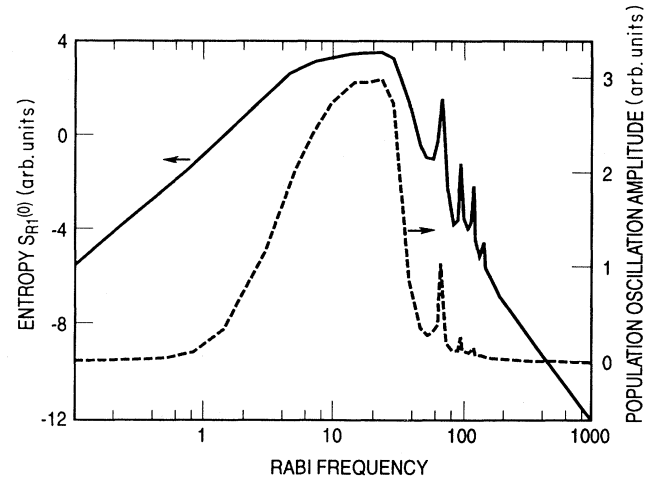

FIG. 7. Bloch-space-attractor entropy (solid line) and amplitude of population oscillations (dashed line) versus Rabi frequency. Note the exact coincidence of the Rabi resonances and the entropy enhancements.

weak-field conditions. Note though, that superimposed on the gradually changing entropy background of Fig. 6 are sharp, resonancelike entropy increases. These entropy resonances occur at *precisely* the same Rabi frequencies as do the Rabi resonances. The correlation between the entropy and Rabi resonances is extremely robust: it is apparent when variations in the $S_{R1}(\epsilon)$ versus Rabi frequency are viewed, as well as when the Bloch-vector trajectories are analyzed in the rotating frame. Furthermore, for a single phase modulation frequency the entropy's dependence on Rabi frequency is dominated by a single resonance feature, again occurring at the same Rabi frequency as the anticipated Rabi resonance [9]. These results show for the first time that Rabi resonances are more than simple increases in the amplitude of population oscillations. Rabi resonances are intimately associated with changes in the system's overall dynamics, signaling increased complexity or "disorder" in the atom's response to the field.

IV. SUMMARY AND CONCLUSIONS

We have examined the population oscillation amplitudes, quantum system attractors, and Renyi entropies for a two-level atom interacting with an electromagnetic field, whose phase varies in a two-frequency quasiperiodic manner. Significant variations in these quantities are observed as the field strength passes from weak to strong. The Bloch-space attractors assume relatively simple geometrical forms in the instantaneous frame under the limiting cases of both weak (nonadiabatic) and strong (adiabatic) levels of excitation, while in the intermediate regime the trajectories become disordered, apparently displaying a higher degree of complexity. Calculation of the Renyi order-1 entropy for the Bloch-vector trajectories is consistent with a higher degree of complexity in the transition region, and this should be noted in light of recent experiments which demonstrate the difficulty of interpreting resonant phenomena in this regime [17]. The transition region is also characterized by the presence of a number of Rabi resonances: at a number of specific Rabi frequency values, significant increases in the amplitude of population oscillations are observed. Additionally, at these exact same Rabi frequency values, we calculate significant increases in the entropy of Bloch-vector trajectories. A key finding of this study is then that Rabi resonances are more than simple increases in oscillation amplitudes; associated with them are distinct disorder-

ings in the dynamics of the two-level system.

While there are clear variations in the precise response of the atomic system as the field strength is varied, the dynamical systems approach we have employed here clearly reveals an underlying homology in the general nature of this response. Under all levels of excitation, the full 5D quantum system produces attractors that are two dimensional (Hausdorff dimension); more specifically, the response is *always* two-frequency quasiperiodic, homeomorphic to a 2-torus. In the strong-field case, the quasiperiodic quantum system response displays generalized dimensions similar in nature to those associated with the phase of the exciting field. As the system is highly adiabatic under these conditions, with the Bloch vector closely following the effective field, this is perhaps not too surprising. However, since in the instantaneous frame the adiabatic Bloch-space attractors have $D_0 = 2$ (i.e., Hausdorff dimension greater than 0), the full 5D quantum system's attractor geometry should not be interpreted as a trivial consequence of mixing the atomic system with the 2-torus of θ_1 and θ_2. It should of course be recognized that the coincidental equivalence of D_0 values for the full quantum system attractor and the Bloch-space attractors is due to our choice of two incommensurate sinusoids for the phase variation. If, for example, four incommensurate sinusoids had been chosen for the phase variation, then in the adiabatic regime at least we could have expected the full 7D attractor's Hausdorff dimension to also be four. However, the Bloch-space attractor must always have $D_0 \leq 3$.

As a final point, it is worth recognizing that in this work we have relied heavily on the analysis tools of dynamical systems, which are typically reserved for nonlinear problems. The present study demonstrates that these tools, even when applied to an inherently linear quantum-mechanical system, supply new insights into that system's interactions. Specifically, in this work these tools have allowed us to uncover a homology with regards to an atom's interaction with a phase varying field, and they have allowed us to demonstrate that atomic systems become disordered at Rabi resonances.

[1] P. W. Milonni, J. R. Ackerhalt, and M. E. Goggin, Phys. Rev. A **35**, 1714 (1987); in *Lasers, Molecules, and Methods: Advances in Chemical Physics* edited by J. O. Hirschfelder, R. E. Wyatt, and R. D. Coalson (Wiley, New York, 1989), Vol. LXXIII.

[2] Y. Pomeau, B. Dorizzi, and B. Grammaticos, Phys. Rev. Lett. **56**, 681 (1986); R. Badii and P. F. Meier, *ibid.* **58**, 1045 (1987); J. M. Luck, H. Orland, and U. Smilansky, J. Stat. Phys. **53**, 551 (1988); S. Adachi, M. Toda, and K. Ikeda, Phys. Rev. Lett. **61**, 659 (1988); C. C. Gerry and T. Schneider, Phys. Rev. A **42**, 1033 (1990).

[3] T. Geisel, Phys. Rev. A **41**, 2989 (1990).

[4] J. C. Camparo and R. P. Frueholz, Phys. Rev. A **43**, 338 (1991).

[5] R. Loudon, *The Quantum Theory of Light* (Clarendon, Oxford, 1983).

[6] J. A. Glazier and A. Libchaber, IEEE Trans. Circuits Syst. **35**, 790 (1988).

[7] P. Berge, Y. Pomeau, and C. Vidal, *Order Within Chaos* (Wiley, New York, 1984), pp. 54–58.

[8] P. Avan and C. Cohen-Tannoudji, J. Phys. B **10**, 155 (1977).

[9] U. Cappeller and H. Mueller, Ann. Phys. (Leipzig) **42**, 250 (1985).

[10] J. C. Camparo and R. P. Frueholz, Phys. Rev. A **38**, 6143 (1988).

[11] K. Pawelzik and H. G. Schuster, Phys. Rev. A **35**, 481 (1987).

[12] K. Falconer, *Fractal Geometry* (Wiley, New York, 1990), Chaps. 6 and 8.

[13] F. J. Romeiras and E. Ott, Phys. Rev. A **35**, 4404 (1987).

[14] H. G. E. Hentschel and I. Procaccia, Physica D **8**, 435 (1983).

[15] P. Grassberger and I. Procaccia, Physica D **9**, 189 (1983).

[16] K. Denbigh, *The Principles of Chemical Equilibrium* (Cambridge University Press, London, 1971), Chap. 11.

[17] J. C. Camparo and C. M. Klimcak, Opt. Commun. **91**, 343 (1992).